frontiers | Frontiers in Cellular and Infection Microbiology

TYPE Original Research
PUBLISHED 12 November 2024
DOI 10.3389/fcimb.2024.1477463

OPEN ACCESS

EDITED BY
Justyna Karkowska-Kuleta,
Jagiellonian University, Poland

REVIEWED BY
Jarrod R. Fortwendel,
University of Tennessee Health Science Center, United States
Sukhvinder Singh,
Wayne State University, United States

*CORRESPONDENCE
Kevin K. Fuller
kkf18@pitt.edu

†PRESENT ADDRESS
Manali M. Kamath,
Department of Ophthalmology, University of Pittsburgh School of Medicine, Pittsburgh, PA, United States
Kevin K. Fuller,
Department of Ophthalmology, University of Pittsburgh School of Medicine, Pittsburgh, PA, United States

RECEIVED 07 August 2024
ACCEPTED 21 October 2024
PUBLISHED 12 November 2024

CITATION
Kamath MM, Adams EM, Lightfoot JD, Wells BL and Fuller KK (2024) The mammalian Ire1 inhibitor, 4μ8C, exhibits broad anti-*Aspergillus* activity *in vitro* and in a treatment model of fungal keratitis. *Front. Cell. Infect. Microbiol.* 14:1477463. doi: 10.3389/fcimb.2024.1477463

The mammalian Ire1 inhibitor, 4μ8C, exhibits broad anti-*Aspergillus* activity *in vitro* and in a treatment model of fungal keratitis

Manali M. Kamath[1†], Emily M. Adams[2], Jorge D. Lightfoot[2], Becca L. Wells[1] and Kevin K. Fuller[1,2,3*†]

[1]Department of Microbiology and Immunology, University of Oklahoma Health Sciences Center, Oklahoma City, OK, United States, [2]Department of Ophthalmology, University of Oklahoma Health Sciences Center, Oklahoma City, OK, United States, [3]Department of Ophthalmology, University of Pittsburgh School of Medicine, Pittsburgh, PA, United States

Objective: The fungal unfolded protein response consists of a two-component relay in which the ER-bound sensor, IreA, splices and activates the mRNA of the transcription factor, HacA. Previously, we demonstrated that *hacA* is essential for *Aspergillus fumigatus* virulence in a murine model of fungal keratitis (FK), suggesting the pathway could serve as a therapeutic target. Here we investigate the antifungal properties of known inhibitors of the mammalian Ire1 protein both *in vitro* and in a treatment model of FK.

Methods: The antifungal activity of Ire1 inhibitors was tested against conidia of several *A. fumigatus* isolates by a broth microdilution assay and against fungal biofilm by XTT reduction. The influence of 4μ8C on *hacA* mRNA splicing in *A. fumigatus* was assessed through gel electrophoresis and qRT-PCR of UPR regulatory genes. The toxicity and antifungal profile of 4μ8C in the cornea was assessed by applying drops to uninfected or *A. fumigatus*-infected corneas 3 times daily starting 4 hours post-inoculation. Corneas were evaluated daily through slit-lamp imaging and optical coherence tomography, or at endpoint through histology or fungal burden quantification via colony forming units.

Results: Among six Ire1 inhibitors screened, the endonuclease inhibitor 4μ8C displayed the strongest antifungal profile with an apparent fungicidal action. The compound both blocked conidial germination and hyphal metabolism of *A. fumigatus* Af293 in the same concentration range that blocked *hacA* splicing and UPR gene induction (60-120 μM). Topical treatment of sham-inoculated corneas with 0.5 and 2.5 mM 4μ8C did not impact corneal clarity, but did transiently inhibit epithelialization of corneal ulcers. Relative to vehicle-treated Af293-infected corneas, treatment with 0.5 and 2.5 mM drug resulted in a 50% and >90% reduction in fungal load, respectively, the latter of which corresponded to an absence of clinical signs of infection or corneal pathology.

Conclusion: The *in vitro* data suggest that 4μ8C displays antifungal activity against *A. fumigatus* through the specific inhibition of IreA. Topical application of the compound to the murine cornea can furthermore block the establishment of infection, suggesting this class of drugs can be developed as novel antifungals that improve visual outcomes in FK patients.

KEYWORDS

fungal keratitis, IRE1 inhibitors, 4μ8C, *Aspergillus fumigatus*, antifungals

1 Introduction

Fungal infections of the cornea are an ophthalmologic emergency and represent a leading cause of ocular morbidity and unilateral blindness worldwide (Thomas, 2003; Cabrera-Aguas et al., 2022). This disease entity, called fungal keratitis (FK), typically affects otherwise healthy individuals that are inoculated with fungal spores or hyphae through ocular trauma or contact lens wear (Acharya et al., 2017; Atta et al., 2022). Even with the current standard of treatment, which includes topical application of natamycin or voriconazole, 40-60% of all FK cases result in corneal perforation and/or the need for corneal transplantation (Lalitha et al., 2006; Ansari et al., 2013). One approach to the development of novel antifungals for FK, or indeed any clinical context, is a biologically-informed one that involves two key steps: first, the identification of a fungal protein/pathway that is essential for growth or virulence in a relevant disease model and, second, identification of a small molecule(s) that inhibits protein function and improves disease outcome in the model without toxicity to the host. In the context of this study, we and others have previously identified the unfolded protein response (UPR) as a critical regulator of *Aspergillus fumigatus* virulence in both pulmonary and corneal infection models, and now seek to develop inhibitors of the pathway as novel antifungals (Richie et al., 2009; Feng et al., 2011; Kamath et al., 2023).

The mammalian UPR consists of three separate but partially redundant signaling branches – IRE1, ATF6, and PERK - where the Ire1 branch is the most highly conserved across the eukaryotes and is the only one found in the fungi (Ron and Walter, 2007; Zhang et al., 2016; Sircaik et al., 2021; Verchot and Pajerowska-Mukhtar, 2021; Ishiwata-Kimata and Kimata, 2023). In *A. fumigatus*, the Ire1 ortholog (IreA) is an ER-bound transmembrane protein comprised of a luminal sensory domain and two cytosolic domains that propagate the signal to the nucleus (Richie et al., 2009; Richie et al., 2011). More completely, the rapid accumulation of misfolded proteins in the ER lumen promotes the oligomerization of IreA within the membrane. This clustering triggers the trans-autophosphorylation of the kinase domain and subsequent activation of the endoribonuclease domain which then splices an unconventional intron from its only known client mRNA, *hacA*. The spliced *hacA* isoform encodes a bZIP transcription factor, HacA, which regulates genes not only involved directly in protein folding homeostasis (e.g. chaperones and foldases), but also genes involved in primary and secondary metabolism that altogether promote adaptation to stressful environments (Cox and Walter, 1996; Sidrauski and Walter, 1997; Richie et al., 2009; Kamath et al., 2023). Recently, we demonstrated that a *hacA* deletion mutant of *A. fumigatus* (Af293 background) is viable under normal growth conditions but is unable to establish infection in a murine model of FK (Kamath et al., 2023). Surprisingly, we were unable to isolate an *ireA* deletant in Af293 and repression of the gene using a tetracycline regulatable promoter blocks hyphal growth (Kamath et al., 2023). Not only does this indicate that IreA regulates fungal growth beyond its influence of HacA, but it pragmatically suggests the protein could serve as an ideal target for antifungal intervention.

Several small molecules are known to inhibit the mammalian Ire1 kinase or endonuclease domains and, consistent with the UPR's role in regulating cellular homeostasis, display anti-proliferative effects in various cell culture or *in vivo* cancer models, including those related to hepatocellular carcinoma, acute myeloid leukemia, triple negative breast cancer, and multiple myeloma (Papandreou et al., 2011; Mimura et al., 2012; Sun et al., 2016; Logue et al., 2018; Pavlović et al., 2020). Recently, Guirao-Abad and colleagues demonstrated that one such compound, the coumarin derivative 4-methyl umbilliferone 8-carbaldehyde (4μ8C), inhibits the endonuclease activity of *A. fumigatus* IreA and consequently the downstream expression of canonical HacA-dependent genes in the setting of acute ER stress (Guirao-Abad et al., 2020). The utility of 4μ8C or other Ire1 inhibitors as clinically useful antifungals, however, has not been explored. In this study, we assess the intrinsic antifungal activity of six Ire1-targeting drugs against common laboratory and corneal isolates of *A. fumigatus*, as well as the ability of the most broadly active compound, 4μ8C, to influence disease outcomes in a murine model of FK.

2 Materials and methods

2.1 Chemical reagents used in the study

All IRE1 inhibitors were prepared in dimethyl sulfoxide (DMSO) and stored at -80°C until use. 50 mM stock of IRE1

inhibitor III, 4μ8C (#412512 - MilliporeSigma, MA, USA), 50 mM Sunitinib (HY-10255A – MedChemExpress, NJ, USA), 10 mM Z4P (HY-153773 – MedChemExpress, NJ, USA), 10 mM STF-083010 (HY-15845 – MedChemExpress, NJ, USA), 10 mM KIRA6 (HY-19708 – MedChemExpress, NJ, USA) and 10 mM HY-114368 (HY-15845 – MedChemExpress, NJ, USA) were used. DL-Dithiothreitol (#0281 DTT- VWR, PA, USA) was prepared at 1 M concentration in sterile PBS.

2.2 Strains and growth conditions

The FK1 and FK2 *A. fumigatus* isolates are from fungal keratitis patients at the University of California at San Francisco-Proctor Foundation. An Af293 derivative strain that constitutively expresses the *mcherry* protein (Af293::*PgpdA-mcherry-hph*) was used throughout this study (Kamath et al., 2023; Lightfoot et al., 2024). Strains were maintained on glucose minimal media (GMM) containing 1% glucose, Clutterbuck salts, and Hutner's trace elements, 10 mM ammonium tartrate (GMM) at pH 6.5 (Cove, 1966). To test the effect of the IRE1 inhibitors on the different *Aspergillus* strains, conidia were inoculated into GMM broth to a final density of 1x 10^6/mL against a concentration gradient of drug (0 - 480 μM) and incubated at 35°C. After 72 h, the minimum inhibitory concentration (MIC) was recorded by visually inspecting the plate and looking for the growth of the fungi under the microscope. To assess the fungicidal effect of the IRE1 inhibitors, a broth microdilution assay was set up as described above and incubated at 35°C for 72 h. 100 μL aliquots from wells in which germination was inhibited were then spread across yeast extract, peptone, dextrose (YPD) plates and incubated at 35°C for 24 h prior to the enumeration of colony-forming units (CFU). To assess biofilm metabolic activity, the XTT metabolic assay was performed as described previously (Pierce et al., 2008). XTT buffer was prepared at a stock of 0.5 mg/mL and menadione at 10 mM in 100% acetone (final conc. 1 μM). For this assay, 10^6 conidia/mL were inoculated in GMM in 96-well plate and incubated at 35°C for 24h to form hyphae followed by treatment with 4μ8C (0 – 240 μM) for 2 h. Next, 100 μL of an XTT-menadione mixture was added to each test well and incubated further for 2 h at 35°C. Supernatants from each well (75 μL) were assayed at 490 nm.

2.3 RT-PCR analyses

Fungal cultures were grown overnight at 35°C in GMM in 6-well plates were treated with a concentration gradient of 4μ8C (0 – 120 μM) for 2 h followed by treatment with 10 mM DTT or vehicle for 2 h. RNA was then extracted from these cultures using RNeasy Mini kit (#74106 Qiagen, Germany) followed by DNase treatment using the DNase I kit (Millipore Sigma, Massachusetts, USA). The Nanodrop 2000 (Thermo Fisher Scientific, Massachusetts, USA) was used to assess the quantity and quality of the RNA. Subsequently, the RNA was standardized for cDNA conversion utilizing the ProtoScript II First Strand cDNA Synthesis Kit (New England Biolabs, Massachusetts, USA) following the provided protocol. To visualize *hacA* splicing, the coding sequencing (spanning the predicted 20 bp unconventional intron) was amplified and resolved by electrophoresis (3% agarose gel at 40 V for 10 h) as previously described (Kamath et al., 2023). For qRT-PCR analysis, Luna Universal qPCR master mix (SYBR green; NEB, USA) was used on the QuantStudio 3 Real-Time PCR System (Thermo Fisher Scientific, Massachusetts, USA), and the analysis was conducted with QuantStudio Design and Analysis Software v1.5.2. Fold-expression changes were computed using the 2-ΔΔCt method, followed by analysis using MS-Excel. The primers used to amplify *hacA*, *bipA* and *pdiA* in this assay are the same as previously published (Guirao-Abad et al., 2020; Kamath et al., 2023).

2.4 Animals

Inoculum: 5x10^6 conidia were incubated in 20 ml YPD at 35°C for approximately 4 h until mostly swollen. Biomass was collected, washed 4x with PBS, and resuspended in 500 μL PBS, adjusting volumes to normalize strains to 0.8 at OD 360 nm. Infections: 6-8-week-old C57B6/6J (Jackson Laboratory) received intraperitoneal immunosuppression with 100 mg/kg Depo-Medrol (Zoetis, USA) on day -1. On day 0, mice were anesthetized using 100 mg/kg ketamine and 6.6 mg/kg xylazine by IP injection, and their right eyes abraded to a 1 mm diameter using Algerbrush II. Fungal inocula (5 μL) were applied to ulcerated eyes and removed with a Kimwipe after 20 minutes. The mice also received Buprenorphine SR (1 mg/kg) which was administered subcutaneously. Contralateral eyes remained uninfected per ARVO guidelines. For controls, we used algerbrushed sham-infected and untouched eyes. Micron IV slit-lamp (Phoenix Research Labs Inc., CA, USA) was used to monitor mice daily post-inoculation (p.i.) up to 72 h. This procedure was performed while the mice were anesthetized with isoflurane. Anterior segment spectral-domain optical coherent tomography (OCT) measured corneal thickness at 48 and 72 h p.i. using a 4x4 mm image using 12 mm telecentric lens from Leica Microsystems (IL, USA). The reference arm was set to 885 according to the manufacturer's calibration instruction. Image analysis was conducted using the InVivoVue diver software. Corneal thickness quantification involved measuring an 11x11 spider plot covering the entire eye, and an average of 13 readings were obtained. Fluorescein imaging: Corneal fluorescein staining was performed to test the rate of healing of the abraded epithelium post treatment with DMSO or 4μ8C. AK-Fluor 10% fluorescein solution (Akorn, IL, USA) diluted 1:100 was applied to the corneas in isoflurane-anesthetized mice using a cotton swab and excess was wiped off and imaged using a slit-lamp Micron (Phoenix Research Labs Inc., CA, USA). Histopathological analysis: Control eyes were harvested after 72 h and fixed with 10% neutral buffered formalin for 24 h followed by 70% ethanol until they were further processed. 5 μm thick sections of the eyes were stained with Hematoxylin and eosin (H&E) to evaluate host inflammatory response after treatment with DMSO or 4μ8C. Fungal burden determination: Corneas were dissected in a sterile manner, homogenized using a collagenase buffer at a concentration of 2 mg/ml, and then 100 μl aliquots were plated in triplicate on inhibitory mold agar (IMA)

plates. The number of colony-forming units (CFU) per cornea was assessed after 24 h of incubation at 35°C. Clinical scoring: Micron images were randomized and scored (0 to 4 scale) for clinical pathology by reviewers not involved with the experiment based on previously established criteria, including surface regularity, area of opacification, and density of opacification (Zhao et al., 2009). Topical Treatments: For the topical treatments of sham or Af293-inoculated corneas, animals were anesthetized using isoflurane and a 5 µL drop of the compound (or DMSO as a vehicle control) was applied to the ocular surface. The animals were kept under anesthesia for 10 minutes with the drop in place before being returned to their cage. The treatment schedule varied slightly across experiments (see the corresponding figure legends), but generally consisted of one treatment on the day of inoculation (4 h p.i.), three treatments (4 h apart) at 1 and 2 days p.i., and one treatment at 3 days p.i., just prior to imaging and removal of the eyes for histological or fungal burden analysis. In the case of the fluorescein experiments, the animals received three treatments 3 days p.i.

2.5 Statistical analyses

All statistical analyses were performed using GraphPad Prism 10 version 10.2.0. The specific tests used for each experiment are described in the corresponding figure legends.

3 Results

3.1 Ire1 endonuclease inhibitors display antifungal activity against *Aspergillus fumigatus* laboratory strains and clinical isolates

We first predicted that Ire1 inhibitors would display *in vitro* antifungal activity against Af293 and potentially other *A. fumigatus* strains in which IreA influences fungal growth and or viability. We began by screening the activity of six commercially available Ire1 inhibitors – including four kinase domain inhibitors (Sunitinib, Z4P, KIRA6, KIRA8) and two endonuclease domain inhibitors (4µ8C, STF-083010) (Supplementary Figure 1) – in a broth microdilution assay. Four *A. fumigatus* strains were tested in the screen, including the well-studied Af293 and CEA10 strains (both pulmonary isolates) and two uncharacterized corneal isolates from fungal keratitis patients, designated here as FK1 and FK2 (Bertuzzi et al., 2021). No inhibitory activity was observed with any of the four kinase inhibitors even at the highest tested concentration (Supplementary Figure 2), suggesting that these compounds either do not adequately accumulate within the fungal cell, they do not have high affinity for the *A. fumigatus* kinase domain, or the domain itself is not essential for *A. fumigatus* growth in these isolates. By contrast, both endonuclease inhibitors fully blocked conidial germination, with 4µ8C and STF-083010 exhibiting comparable MICs against Af293 and FK1, and 4µ8C displaying overall lower MICs against CEA10 and FK2 (Figure 1A). To gain some insight into whether their inhibitory action was fungistatic or fungicidal, the microtiter assay was repeated with Af293 and, following 72 h incubation in the presence of drug, aliquots from wells in which germination was inhibited (120-480 µM) were spread onto drug-free YPD plates and incubated for an additional 24 h (Figure 1B). Whereas cultures inhibited by STF-083010 all yielded fungal colonies upon sub-culture, all plates corresponding to 4µ8C inhibition remained sterile. These results suggest that 4µ8C is either more potently fungicidal than STF-083010 or that its repressive action, perhaps as a reflection of target binding affinity, is stronger (Figure 1B). To determine if 4µ8C can similarly affect fungal hyphae (i.e. the tissue invasive form), an XTT reduction assay was performed on mycelia/biofilms cultured overnight in static culture and subsequently treated with the drug for 2 h. As shown in Figure 1C, the 120 and 240 µM treatments resulted in a markedly reduced or undetectable metabolic activity, respectively, altogether indicating that a similar concentration of drug is inhibitory and potentially fungicidal against both the conidia and hyphae of *A. fumigatus*. Since 4µ8C provided the best antifungal profile, both in terms of its MIC across the strains and its possible fungicidal action, we decided to prioritize that compound for downstream characterization.

3.2 The antifungal activity of 4µ8C corresponds to an inhibition of Ire1 activity in Af293

In biochemical assays, 4µ8C forms a Schiff base with distinct lysine residues in both the Ire1 kinase and endonuclease domains, but only inhibits the activity of the latter in treated cells (Cross et al., 2012). This lysine is conserved in the *A. fumigatus* IreA endocnuclease domain, as is the influence of the drug on *hacA* splicing in the AfS28/D141 background (Guirao-Abad et al., 2020). We reasoned that if the antifungal action of 4µ8C against Af293 were attributable to an 'on-target' effect, then there would be a correspondence between the fungicidal MIC (ranging from 60 to 120 µM) and the inhibition of IreA function. To explore this, fungal mycelia/biofilms were developed in GMM static culture overnight, subsequently pretreated with DMSO (vehicle) or various concentrations of 4µ8C for 2 h, and finally stimulated with 10 mM DTT for an additional 2 h. Samples treated with neither 4µ8C nor DTT served as a control. The splicing status of *hacA* was then assessed by RT-PCR and gel electrophoresis as previously described (Kamath et al., 2023). As expected, treatment with DTT alone resulted in an observable accumulation of the spliced/induced *hacA* product (*hacA*^{i}), relative to untreated controls, and the inclusion of 30 µM 4µ8C did not have an impact on this response. By contrast, the *hacA*^{i} splice form was completely absent in both the 60 and 120 µM 4µ8C treated samples, thus establishing a putative connection between IreA function and fungal cell metabolism or viability (Figure 2A; Supplementary Figure 3). Sequencing of these end-point PCR products revealed that the canonical (spliceosomal) intron at the 5' end of the *hacA* mRNA was absent in all samples, whereas the 20 bp IreA-targeted (non-canonical) intron was absent only in the DTT-treated fungus in the absence of 4µ8C (Figures 2C, D; Supplementary Figure 3). Finally, in addition to a

10.3389/fcimb.2024.1477463

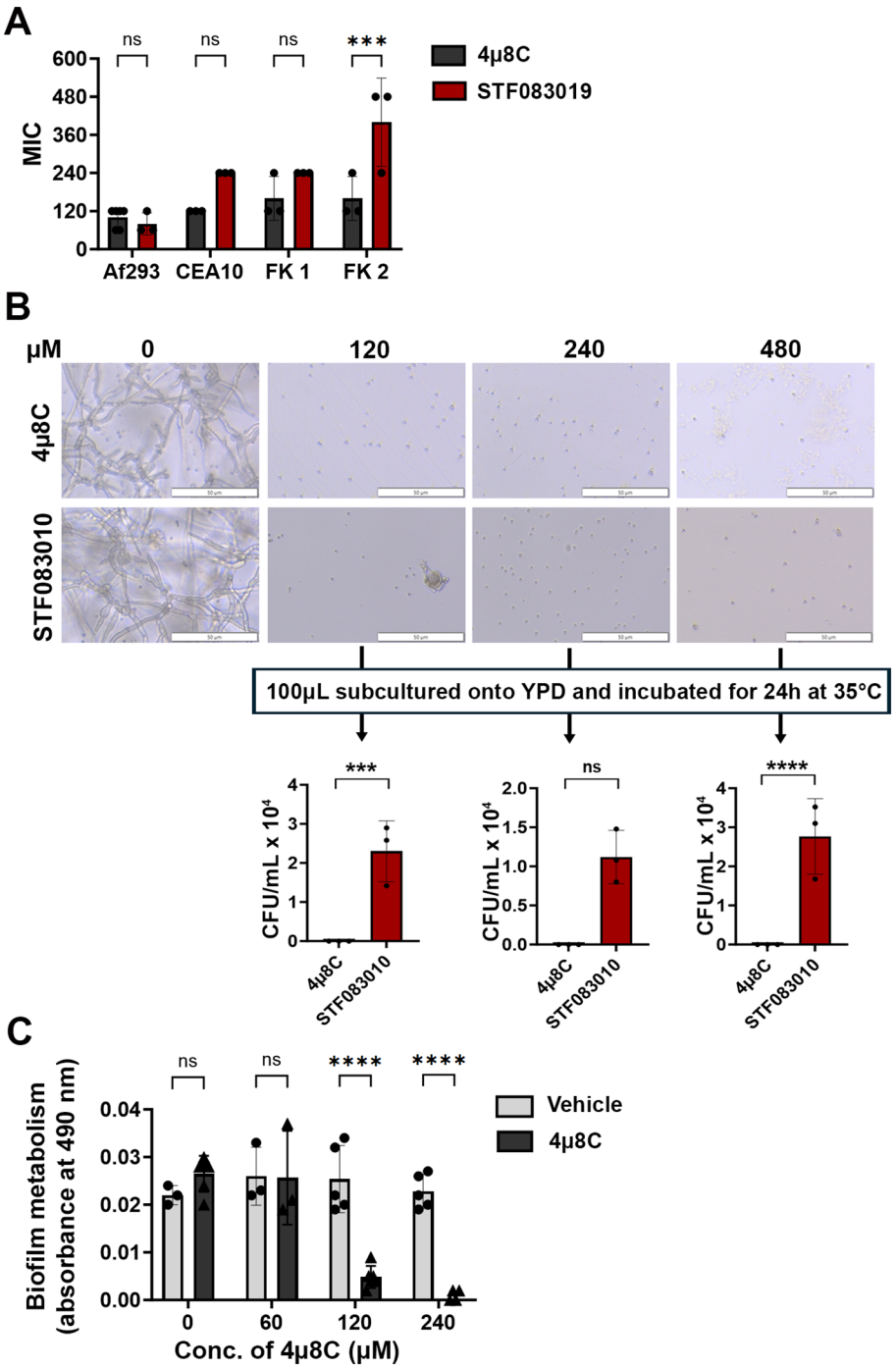

FIGURE 1
4μ8C displays antifungal activity against *A. fumigatus* conidia and hyphae *in vitro*. **(A)** Conidia of the indicated strains were inoculated into GMM broth containing drug and incubated for 72 h at 35°C. The minimal inhibitory concentration (MIC) for at least three independent experiments are plotted and groups were compared by Two-way ANOVA, ***<0.0005. **(B)** Following 72 h incubation of Af293 in a broth microdilution assay described in panel **(A)**, 100 μL aliquots were spread onto YPD plates and incubated for 24 h at 35°C. The data reflect the mean colony counts from triplicate wells of a single broth microdilution experiment and the groups were compared by Two-way ANOVA, ***<0.0005, ****<0.0001. **(C)** Af293 biofilms generated in GMM were treated with vehicle (DMSO) or the indicated concentration of 4μ8C for 2 h at 35°C. Metabolic activity was measured by XTT reduction. The data reflect the mean of 490 nm absorbance (± SD) of triplicate wells in single experiment and groups were compared by Two-way ANOVA **** <0.0001. Similar results were recapitulated across three independent experiments.

block in *hacA* splicing, we further observed that 60 μM blocked the DTT-mediated induction *hacA* message as well as the steady-state mRNA of two known HacA-regulated transcription factors, BipA and PdiA (Guirao-Abad et al., 2020) (Figure 2B). Taken together, these results support a model in which 4μ8C blocks UPR signaling in *A. fumigatus*, and by extension fungal metabolism and growth, through a specific action on IreA endonuclease activity, rather than a broad inhibition of mRNA processing by the spliceosome.

10.3389/fcimb.2024.1477463

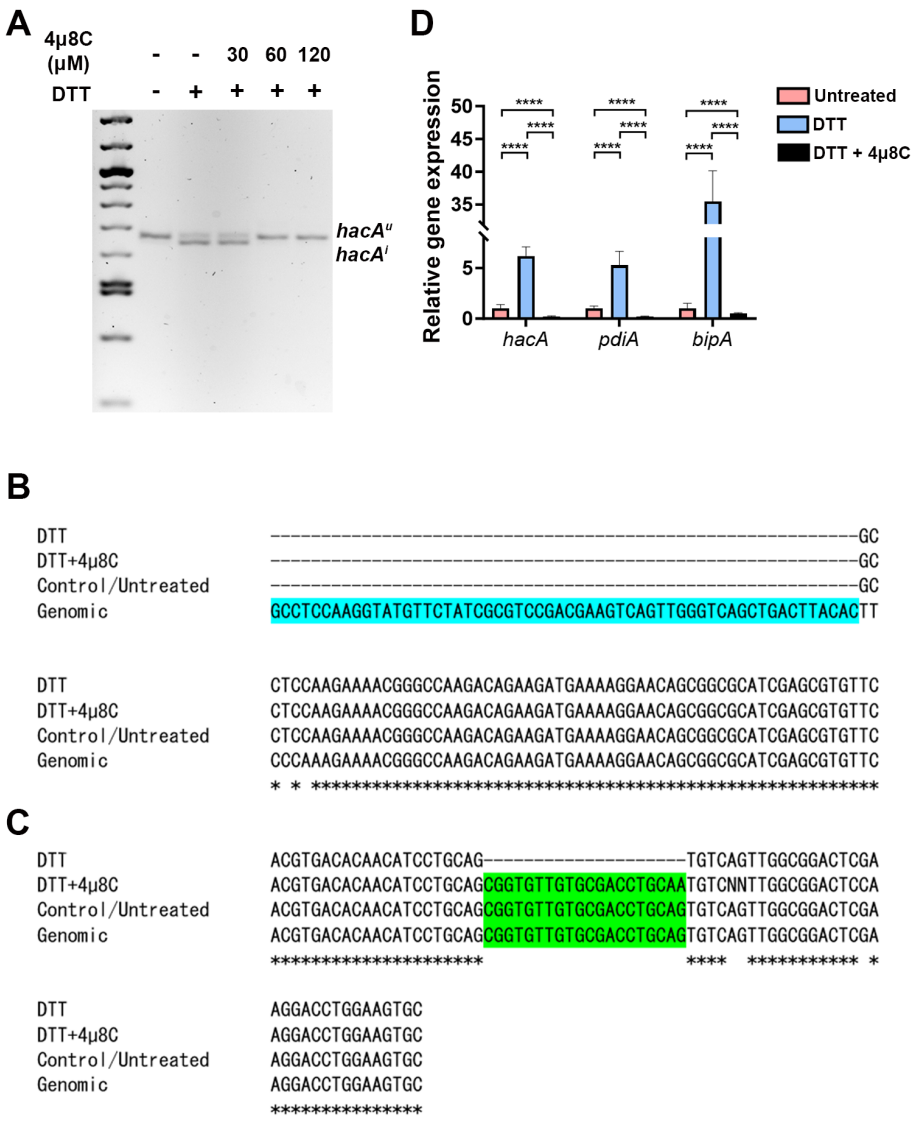

FIGURE 2
The antifungal activity of 4μ8C corresponds to an inhibition of IreA activity in Af293. Af293 biofilms generated overnight in GMM were pre-treated with 4μ8C or DMSO for 2 h and subsequently spiked with 10 mM DTT and incubated for an additional 2 h prior to total RNA isolation and cDNA synthesis. **(A)** The full-length *hacA* message was amplified and the *hacA*^{U} (uninduced: 665 bp) and *hacA*^{I} (induced: 645 bp) products were resolved by gel electrophoresis. The end point *hacA* PCR products were sequenced and a CLUSTAL multiple sequence alignment was performed in the regions spanning the canonical/spliceosome intron highlighted in blue **(B)** and the IreA-targeted non-canonical intron highlighted in green **(C)**. **(D)** qPCR was performed on total *hacA* as well as two chaperone encoding genes, *bipA* and *pdiA*. The qPCR data reflect the mean $2^{\Delta\Delta Ct}$ calculations for triplicate fungal samples from a single experiment and groups were compared by Two-way ANOVA, ****<0.0001. Similar results were observed in an independent experiment.

3.3 High dose 4μ8C treatment does not impact corneal clarity but does transiently inhibit re-epithelialization

We were next interested in exploring the *in vivo* antifungal activity of 4μ8C in a murine model of FK, but first had to consider the concentration to test. Ophthalmic antifungal formulations tend to be highly concentrated to facilitate sufficient accumulation of the drug within the dense collagen matrix of the cornea, particularly in the face of rapid dilution and drainage of the drug at the ocular surface. For example, the *in vitro* MIC for natamycin against most *Aspergillus* isolates ranges between 2-32 μg/mL but is administered at 500-25,000X this concentration in the form of hourly 50 mg/mL (75 mM) drops. Similarly, voriconazole drops are often formulated at 1 mg/mL (28 mM), where the *in vitro* MIC for most *A. fumigatus* isolates is 0.25-4 μg/mL (Sun et al., 2014). Thus, while testing the highest concentration of 4μ8C that its solubility permits (132.24 mM) would be desirable, we had to further consider that the impact of the drug on corneal tissue homeostasis has not been explored. We therefore began by testing the ocular toxicity profiles of two relatively conservative 4μ8C concentrations, 0.5 and 2.5 mM, which correspond to approximately 5X and 40X the *in vitro* antifungal MIC, respectively.

The two drug concentrations were evaluated in sham model of FK previously developed by our group, which involves the

10.3389/fcimb.2024.1477463

generation of an epithelial ulcer ahead of fungal inoculation, or in this case, ulceration without the addition of fungus (Sun et al., 2016; Kamath et al., 2023). Each treatment consisted of a 5 µL drop of 4µ8C or vehicle (DMSO) applied to the corneal surface up to three times daily per the schedule described on the corresponding figure legends and methods. Corneas were tracked daily by slit-lamp imaging to assess corneal clarity and ocular surface regularity, as well as by optical coherence tomography (OCT) to measure corneal thickness and assess gross morphology. Corneas were then resected at 72 h post-ulceration for histological analysis with H&E staining. Relative to the vehicle control group, neither 4µ8C concentration had an observable impact on corneal clarity or corneal thickness, suggesting the drug did not lead to acute inflammation or edema (Figures 3A, B; Supplementary Figures 4A, B). Interestingly, histology revealed that whereas the epithelium of vehicle-treated corneas had reformed, those treated with either concentration of 4µ8C still appeared ulcerated (Figure 3C; Supplementary Figure 4C). To evaluate this further, we replicated the experiment and followed re-epithelialization (wound healing) longitudinally with fluorescein staining. Briefly, an intact corneal epithelium precludes the entry of the stain into the underlying tissue, thus giving a negative signal on fluorescence slit-lamp imaging; by contrast, ulcerated eyes give rise to diffuse yellow-green staining of the stromal layer. As opposed to the vehicle-treated eyes, which fully precluded stromal staining within 24 h post-ulceration, the 4µ8C-treated group remained positive for the duration of the 72 h treatment. We observed, however, that the corneas were fully healed within 3 days of stopping the 4µ8C treatment, suggesting that the

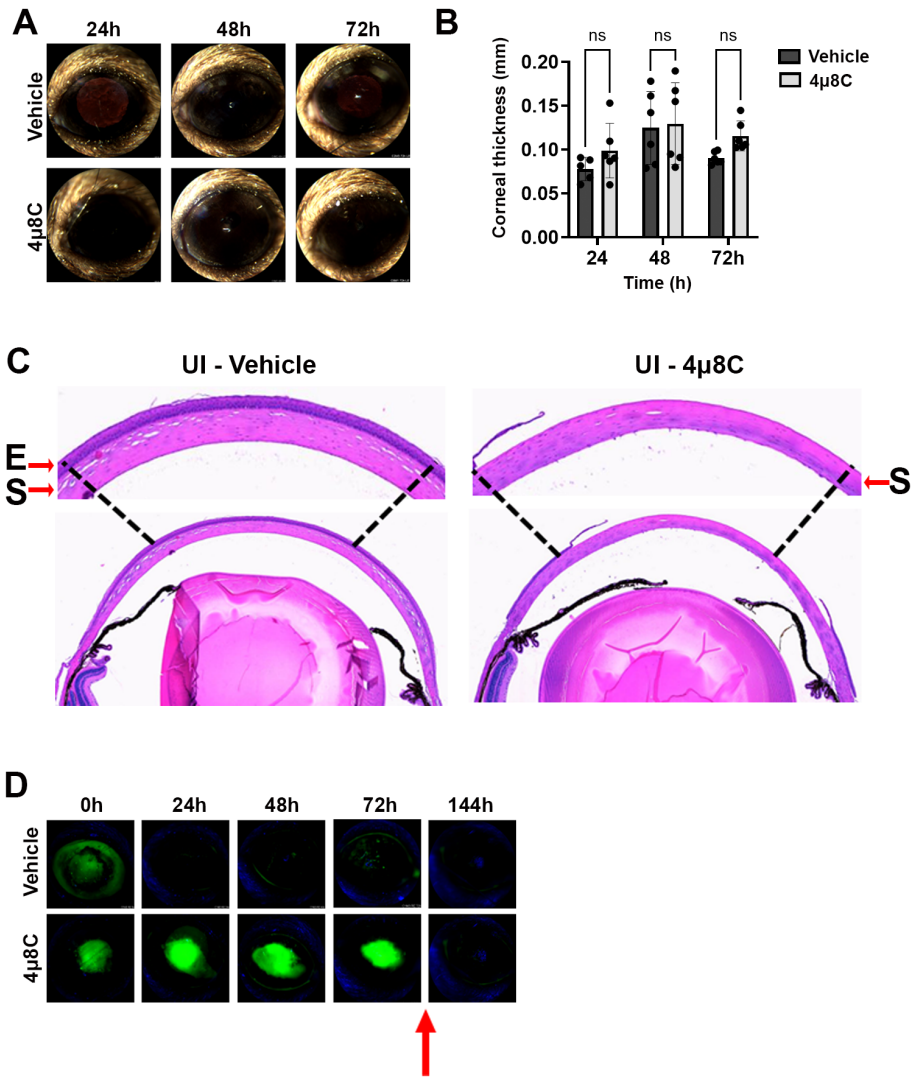

FIGURE 3
High dose 4µ8C treatment does not impact corneal clarity but does transiently inhibit re-epithelialization. Sham-inoculated (UI) corneas were treated with topical drops of 2.5 mM 4µ8C or vehicle (DMSO), once on the day on ulceration (4 h p.i.), three times (4 h apart) the following three days. **(A)** Representative external images taken each day post-ulceration. **(B)** Corneal thickness was measured daily based on OCT images (n = 6/group). Groups were compared by Two-way ANOVA; **(C)** Representative histological (H&E) sections taken at 72 h post-ulceration; 400X magnification. The arrows are highlighting the epithelial 'E' and the stromal 'S' layers. **(D)** In a separate experiment, ulcerated eyes were treated as described above and on each day the penetration of fluorescein was imaged by a fluorescent slit-lamp (Micron IV). The red arrow indicates that the treatment was stopped, and the eyes were monitored for an additional three days.

drug has only a transient impact on epithelial cell proliferation (Figure 3D; Supplementary Figure 4D). Taken together, we concluded that the tested treatment regimens of 4μ8C were minimally toxic to the murine cornea and suitable for evaluation in a treatment model of FK.

3.4 Topical treatment with 4μ8C blocks fungal growth and disease establishment in a murine model of FK

To test the impact of 4μ8C on fungal growth and disease outcomes during FK, we inoculated ulcerated corneas with swollen conidia of *A. fumigatus* Af293 (day 0) and treated on the same schedule as described above – once on the day of ulceration/inoculation, three times at 24 and 48 h p.i, and once at 72 h p.i. Corneal disease metrics were tracked longitudinally by slit-lamp and OCT as before, but included fungal burden assessment at 72 h by homogenizing and plating corneas for CFU enumeration. We began with the 0.5 mM 4μ8C preparation, where the lack of corneal toxicity on sham/uninfected corneas observed in the previous safety trial was recapitulated. Furthermore, treatment at this concentration resulted in an approximately 50% reduction in fungal load at 3 days p.i. relative to vehicle-treated FK corneas (Supplementary Figure 5A). This reduction in fungal load did not, however, correspond to improved clinical disease scores or reduced corneal thickness at any of the evaluated time points (Supplementary Figures 5B–D), suggesting this treatment regimen is insufficient to block corneal inflammation and tissue damage associated with FK pathology. We next tested the higher (2.5 mM) concentration of 4μ8C in the same manner and observed a >90% reduction in fungal burden at 72 h p.i. that corresponded to an absence of corneal surface disease or cornea swelling at all evaluated time points (Figure 4). These results suggested that the higher 4μ8C dosage led to a rapid corneal sterilization that blocked the establishment of infection and downstream pathology. The relative influence of 0.5 and 2.5 mM 4μ8C on fungal load and disease development was recapitulated across multiple experiments with each concentration.

4 Discussion

The conservation of essential proteins between fungi and mammals is an important barrier to the development of potent antifungals with acceptable host toxicity profiles. On the other hand, existing drugs developed against human proteins, particularly those in the cancer therapeutic pipeline, may display dually useful antifungal properties (Kim et al., 2020). In this report, we demonstrate that the mammalian Ire1 inhibitor 4μ8C, which blocks tumor growth in various pre-clinical models, inhibits the growth of several *A. fumigatus* isolates and can furthermore block the development of FK when applied topically to the corneal surface (Qiu et al., 2013; Stewart et al., 2017; Pavlović et al., 2020). These results underscore the utility of drug repurposing efforts in the battle against medically important fungi, as well as the importance of fungal keratitis as an important experimental platform towards this end.

Our interest in developing Ire1 inhibitors as antifungals was prompted by work in *A. fumigatus* strain Af293, in which an *ireA* deletant could not be isolated and repression of the gene via a regulatable promoter halted growth under standard laboratory conditions (Kamath et al., 2023). Here we demonstrate that 4μ8C fully blocks Af293 germination or hyphal metabolic activity at 60-120 μM, which aligns closely with the drug concentration that inhibits IreA endonuclease activity. Thus, the genetic and pharmacological data are seemingly in agreement and indicate that the antifungal activity of 4μ8C is owed to the "on-target" inhibition of an essential *A. fumigatus* protein: IreA. The possibility of "off-target" effects for 4μ8C cannot be ruled out, however, and may indeed be implicated by two lines of evidence. The first relates to the fact that 4μ8C and STF-083010 inhibit conidial germination at the same concentration, yet the latter can seemingly do so independently of cell death. As these drugs have been shown to inhibit mammalian Ire1 function through the same mechanism (Guirao-Abad et al., 2020), our data support a model in which the greater or faster killing kinetics of 4μ8C is attributable to effects beyond IreA inhibition. In agreement with this idea is work by others that established *ireA* is not an essential gene in an *A.fumigatus* D141 derivative (AfS28), yet 4μ8C can inhibit hyphal metabolism/viability of this strain at concentrations above which block IreA activity (Feng et al., 2011; Guirao-Abad et al., 2020). Thus, while it is possible that 4μ8C inhibits other essential enzymes or metabolic processes that contribute to its *in vitro* antifungal activity, it is also likely that the exact influence of the drug is variable across *A. fumigatus* lineages/isolates. We postulate that some *A. fumigatus* strains, such as Af293, experience a relatively higher level of ER stress during normal growth that renders IreA essential and, by extension, 4μ8C fungicidal. Alternatively, other lineages that include D141 may have recruited alternative signaling pathways that can compensate for IreA loss; in these isolates, 4μ8C would only moderately impact growth *in vitro* until higher (i.e. off-target inducing) concentrations of drug are applied. Such strain heterogeneity with respect to IreA signaling is an ongoing line of investigation in our group. Nevertheless, *ireA* is essential for the virulence of the D141 strain in the setting of invasive pulmonary aspergillosis (Feng et al., 2011), supporting its feasibility in principle as an antifungal target irrespective of fungal background.

We demonstrate that topical application of 2.5 mM 4μ8C (~40x the *in vitro* MIC in GMM) to *A. fumigatus*-infected corneas can block fungal growth and the subsequent development of disease. This effect is dose-dependent as treatment with less concentrated drops (0.5 mM) results in only a 50% reduction in fungal burden and no discernable impact on the rate of disease progression or severity. We believe these findings reflects a non-linear relationship between fungal load in the cornea and clinical pathology, such that 1) a 50% reduction in fungal antigen does not lead to a proportional reduction in the corneal inflammation and opacification or, 2) a 50% reduction in corneal inflammation is simply not clinically appreciable. Moreover, it remains unclear why the 0.5 mM concentration displays incomplete antifungal activity despite being 8X the *in vitro* MIC. We hypothesize that a combination of physical barriers, including rapid drainage from the ocular surface and slow penetration through the stromal collagen matrix, act in

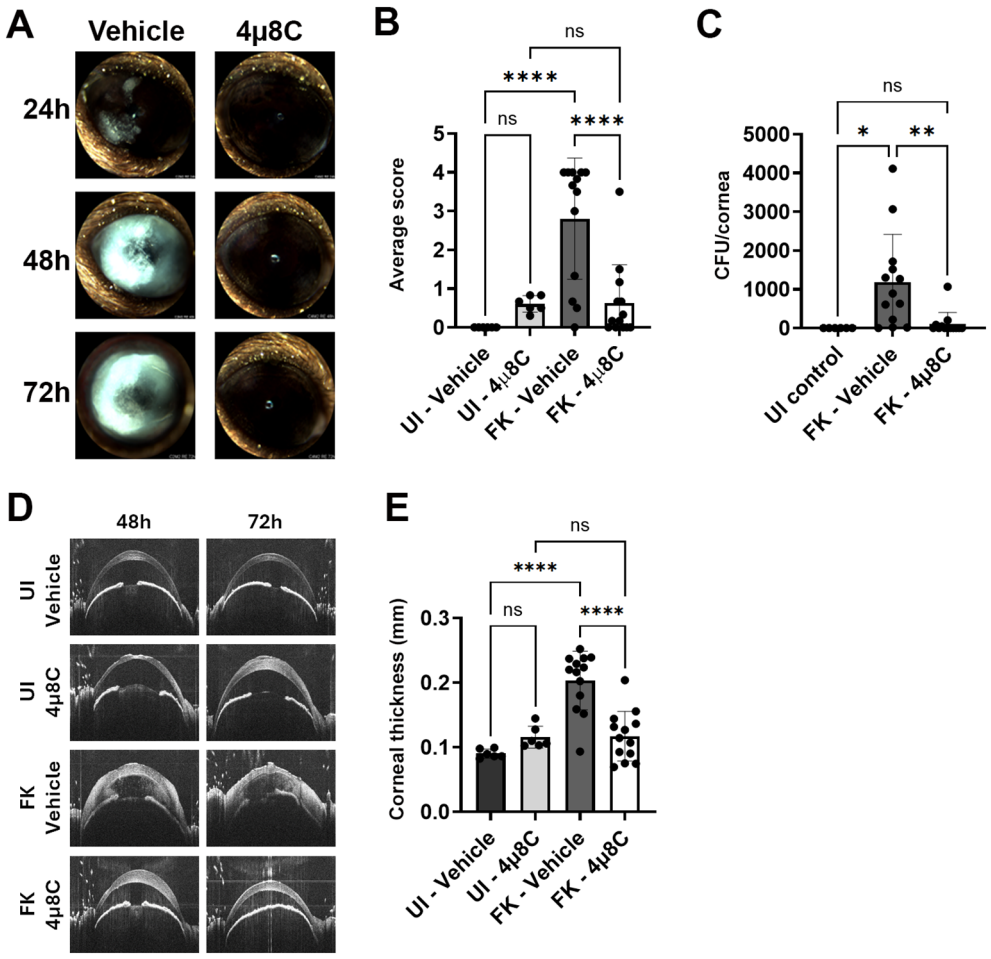

FIGURE 4
Topical treatment with 4μ8C blocks fungal growth and disease establishment in a murine model of FK. Sham (UI) or Af293-inoculated (FK) corneas were treated with 2.5 mM 4μ8C or vehicle for up to 72 h p.i. as described in the Figure 3 legend. The data in all panels reflect a pool of two independent experiments (n=6 per UI group; n=13 per FK group). **(A)** Representative external images taken each day p.i. **(B)** Average clinical scores at 72 h p.i.; Groups were compared by Ordinary one-way ANOVA p-value **** <0.0001; **(C)** Fungal burden at 72 h p.i.; Groups were compared by Ordinary one-way ANOVA p-value ** 0.0061, * 0.0173; **(D)** Representative OCT scans of UI and FK corneas treated with 2.5 mM 4μ8C or vehicle at 48 and 72 h p.i. **(E)** Average corneal thickness measured at 72 h p.i.. Groups were compared by Ordinary one-way ANOVA p-value **** <0.0001.

concert with a fungal biological response, such as drug efflux, to ultimately reduce the intracellular concentration of drug with the fungal cell. The fact that an effective antifungal concentration of the drug is achievable through periodic drops alone nevertheless suggests this class of compounds can be further optimized for ophthalmic use.

Beyond the antifungal properties of 4μ8C, it is important to consider the impact of such treatment on various host cell populations as it pertains to FK pathogenesis, disease resolution, or overall ocular health. In the retina, for example, Ire1 signaling plays an important role in photoreceptor homeostasis and tissue-specific genetic ablation promotes photoreceptor degeneration in mice (Massoudi et al., 2023; Zhang et al., 2023). Furthermore, and directly relevant to our study, it has been shown that 4μ8C treatment results in reduced tight junction expression of cultured retinal pigment epithelial cells, which contribute to retinal health in myriad ways, including the formation of the outer blood-retinal barrier (Ma et al., 2016). It is unclear to what extent topical and relatively short-term 4μ8C treatment would impact the back of the eye, but our future studies will track retinal function and anatomy over the course of treatment using electroretinography and OCT, respectively.

From a corneal safety perspective, we note that 4μ8C treatment did not alter corneal clarity or tissue thickness in uninfected controls, suggesting the compound does not promote corneal inflammation or edema, the latter of which can arise upon corneal endothelial dysfunction (Feizi, 2018; Price et al., 2021). We do observe, however, a transient block of corneal re-epithelialization, which is consistent with the known anti-proliferative effects of the compound (Cross et al., 2012; Stewart et al., 2017). While at face value this represents a unwanted side-effect of the drug in healthy eyes, the issue may be less important in infected corneas in which corneal inflammation also blocks re-epithelialization, at least in our model (Kamath et al., 2023; Lightfoot et al., 2024). We further note that a transient impact of the drug on epithelial integrity may actually be clinically useful.

Indeed, a major barrier to corneal penetration of topically applied drugs is the epithelium and, consequently, this cellular layer is often debrided by clinicians to improve drug delivery in the treatment of FK. For example, corneal debridement precedes the topical application of photosensitizers in photodynamic therapy (Altamirano et al., 2012; Li et al., 2018). Thus, the antiproliferative effect of the 4μ8C may actually facilitate drug penetration in ulcerated eyes and promote its antifungal efficacy. Another important consideration is that 4μ8C also inhibits TGFβ-driven fibroblast activation and liver fibrosis *in vivo* (Heindryckx et al., 2016; Pavlović et al., 2020). As myofibroblast transformation and corneal scarring are important long-term complications of FK (Zhou et al., 2019; Menda et al., 2020) (i.e., even if corneal sterilization is achieved), we further reason that 4μ8C treatment alone or in conjunction with other antifungals may improve visual outcomes post-infection. A final and potentially important impact of 4μ8C on the host relates to corneal inflammation. It has been demonstrated that Ire1 activation in various myeloid cell populations promotes pro-inflammatory cytokine secretion in response to *C. albicans* infection in the kidney, and this occurs downstream of Dectin-1 and MyD88 signaling following fungal antigen recognition (Awasthi et al., 2023). Importantly, the genetic or pharmacological inhibition of Ire1 (using a different endonuclease inhibitor not evaluated here), reduces kidney inflammation and promotes mouse survival in a murine model of systemic candidiasis. Concerning the eye, Kumar et al. recently demonstrated that intravitreal injection of 4μ8C blocks the host pro-inflammatory response in a murine model of *Staphylococcus* endophthalmitis due to an Ire1-dependent activation of NK-kB signaling downstream of the Toll-like receptor 2 (Kumar et al., 2020). The consequence of 4μ8C treatment in those experiments was uncontrolled bacterial growth and worsened disease outcomes. However, as fungal growth is also inhibited by the compound, we suspect that 4μ8C may serve as a dual-edged sword that mitigates corneal damage caused by both the fungus and the host response (immunopathogenesis). Though we did not observe an obvious reduction in inflammation upon treatment with 0.5 mM 4μ8C in this study, ongoing work seeks to more directly assess the impact of the drug on the corneal cell response to fungal antigen *in vitro* as well as peripheral cell infiltration *in vivo*.

In summary, the current study serves as an important proof-of-principle for the development of UPR-targeting antifungals. It also highlights the relevance of the corneal model for antifungal development more generally as it allows for the longitudinal tracking of host toxicity and disease development before transitioning into visceral organ or systemic models of infection. Regarding FK, it is important to note that patients typically present to the clinic after the development of clinical signs of disease, including corneal haze or corneal ulcer formation. Thus, while we have demonstrated that 4μ8C can effectively kill *A. fumigatus* on the ocular surface and block disease establishment in our model, future studies will need to investigate treatment efficacy when initiated at later time points post-inoculation. We will further address the antifungal properties, both *in vitro* and *in vivo*, against other FK-relevant fungi, including *Candida albicans* and various *Fusarium* species.

Data availability statement

The original contributions presented in the study are included in the article/Supplementary Material. Further inquiries can be directed to the corresponding author.

Ethics statement

All animal studies were approved by the University of Oklahoma Institutional Care and Use Committee. The studies were conducted in accordance with the local legislation and institutional requirements, and in accordance with the Association for Research in Vision and Ophthalmology (ARVO) guidelines for the use of animals in vision research.

Author contributions

MK: Conceptualization, Data curation, Formal Analysis, Investigation, Methodology, Visualization, Writing – original draft, Writing – review & editing. EA: Data curation, Formal Analysis, Investigation, Writing – review & editing. JL: Data curation, Formal Analysis, Investigation, Writing – review & editing. BW: Data curation, Formal Analysis, Investigation, Writing – review & editing. KF: Conceptualization, Formal Analysis, Funding acquisition, Methodology, Project administration, Resources, Supervision, Writing – original draft, Writing – review & editing.

Funding

The author(s) declare that financial support was received for the research, authorship, and/or publication of this article. This work was supported by the National Institutes of Health (R01EY033866, P20GM134973, T32EY023202) and a Career Development Award from Research to Prevent Blindness (RPB) to KF. Core support to the OUHSC Department of Ophthalmology was further provided through P30EY021725 from NIH and an unrestricted grant from RPB.

Acknowledgments

We thank Mark Dittmar and staff at the Dean McGee Eye Institute (DMEI) Animal Research Facility for animal work support, Linda Boone and Louisa Williams at the DMEI Imaging Core for histology, and the Oklahoma Medical Research Foundation Clinical Genomics Center for Sanger sequencing support. We further thank Dr. Thomas Lietman at the University of California San Francisco for the gift of the FK1 and FK2 *A. fumigatus* isolates.

Conflict of interest

The authors declare that the research was conducted in the absence of any commercial or financial relationships that could be construed as a potential conflict of interest.

The author(s) declared that they were an editorial board member of Frontiers, at the time of submission. This had no impact on the peer review process and the final decision.

Publisher's note

Supplementary material

The Supplementary Material for this article can be found online at: https://www.frontiersin.org/articles/10.3389/fcimb.2024.1477463/full#supplementary-material

SUPPLEMENTARY FIGURE 1
Chemical structure of the drugs screened in this study.

SUPPLEMENTARY FIGURE 2
The Ire1 kinase domain inhibitors do not display antifungal activity *in vitro*. Conidia of the *A. fumigatus* isolates were inoculated into GMM broth containing the 480 μM of the indicated drug and incubated for 72 h at 35°C. Images represent a consistent result observed across three independent experiments.

SUPPLEMENTARY FIGURE 3
Unaltered agarose gel image corresponding to Figure 2. The original/raw ethidium bromide gel image captured from the Alliance Q9 Advanced Chemidoc (Uvitec) imaging platform. The image is unaltered in Figure 2A beyond the cropping of the rightmost two lanes, which correspond to the Af293 gDNA and no-template control amplicons, respectively.

SUPPLEMENTARY FIGURE 4
0.5 mM 4μ8C treatment does not impact corneal clarity but does transiently inhibit re-epithelialization. Sham-inoculated (UI) corneas were treated with topical drops of 0.5 mM 4μ8C or vehicle (DMSO) three times per day (4 h apart) starting on day after ulceration. **(A)** Representative external images taken each day post-ulceration. **(B)** Corneal thickness was measured daily based on OCT images. Groups were compared by Two-way ANOVA; **(C)** Representative histological (H&E) sections taken at 72 h post-ulceration; 400X magnification. The arrows are highlighting the epithelial 'E' and the stromal 'S' layers. **(D)** In a separate experiment, ulcerated eyes were treated as described above and on each day the penetration of fluorescein was imaged by a fluorescent slit-lamp (Micron IV). The red arrow indicates that the treatment was stopped, and the eyes were monitored for an additional three days.

SUPPLEMENTARY FIGURE 5
Treatment with 0.5 mM 4μ8C reduces fungal burden but has no significant impact on clinical disease severity. Af293-inoculated (FK) corneas were treated with topical drops of 0.5 mM 4μ8C or vehicle (DMSO) 3X per day starting on day after ulceration and as described in the methods. The data reflect results from a single experiment (n=4 per UI group; n=8 per FK group). **(A)** Fungal burden at 72 h p.i. Groups were compared by Ordinary one-way ANOVA p-value **** <0.0001, ** 0.0012 (n=3, UI; n=6, FK-vehicle; n=4, FK-4μ8C); **(B)** Representative micron images over the course of the infection. **(C)** Average clinical scores at 72 h p.i. Groups were compared by Ordinary one-way ANOVA, p-value **** <0.0001; **(C)** Corneal thickness measurements at 72 h p.i. Groups were compared by Ordinary one-way ANOVA p-value **** <0.0001, *** 0.0003.

References

Acharya, Y., Acharya, B., and Karki, P. (2017). Fungal keratitis: study of increasing trend and common determinants. *Nepal J. Epidemiol.* 7, 685–693. doi: 10.3126/nje.v7i2.17975

Altamirano, D., Martinez, J., Leviste, K. D., Parel, J. M., and Amescua, G. (2020). Photodynamic Therapy for Infectious Keratitis. *Curr Ophthalmol Rep.* 8, 245–251. doi: 10.1007/s40135-020-00252-y

Ansari, Z., Miller, D., and Galor, A. (2013). Current thoughts in fungal keratitis: Diagnosis and treatment. *Curr. Fungal Infect. Rep.* 7, 209–218. doi: 10.1007/s12281-013-0150-1

Atta, S., Perera, C., Kowalski, R. P., and Jhanji, V. (2022). Fungal keratitis: clinical features, risk factors, treatment, and outcomes. *J. Fungi.* 8 (9), 962. doi: 10.3390/jof8090962

Awasthi, D., Chopra, S., Cho, B. A., Emmanuelli, A., Sandoval, T. A., Hwang, S.-M., et al. (2023). Inflammatory ER stress responses dictate the immunopathogenic progression of systemic candidiasis. *J. Clin. Invest.* 133 (17), e167359. doi: 10.1172/JCI167359

Bertuzzi, M., van Rhijn, N., Krappmann, S., Bowyer, P., Bromley, M. J., and Bignell, E. M. (2021). On the lineage of Aspergillus fumigatus isolates in common laboratory use. *Med. Mycol.* 59, 7–13. doi: 10.1093/mmy/myaa075

Cabrera-Aguas, M., Khoo, P., and Watson, S. L. (2022). Infectious keratitis: A review. *Clin. Exp. Ophthalmol.* 50, 543–562. doi: 10.1111/ceo.14113

Cove, D. J. (1966). The induction and repression of nitrate reductase in the fungus Aspergillus nidulans. *Biochim. Biophys. Acta [Internet].* 113, 51–56. doi: 10.1016/S0926-6593(66)80120-0

Cox, J. S., and Walter, P. (1996). A novel mechanism for regulating activity of a transcription factor that controls the unfolded protein response. *Cell.* 87, 391–404. doi: 10.1016/S0092-8674(00)81360-4

Cross, B. C. S., Bond, P. J., Sadowski, P. G., Jha, B. K., Zak, J., Goodman, J. M., et al. (2012). The molecular basis for selective inhibition of unconventional mRNA splicing by an IRE1-binding small molecule. *Proc. Natl. Acad. Sci.* 109, E869–E878. doi: 10.1073/pnas.1115623109

Feizi, S. (2018). Corneal endothelial cell dysfunction: etiologies and management. *Ther Adv Ophthalmol.* 10, 2515841418815802. doi: 10.1177/2515841418815802

Feng, X., Krishnan, K., Richie, D. L., Aimanianda, V., Hartl, L., Grahl, N., et al. (2011). Haca-independent functions of the ER stress sensor irea synergize with the canonical UPR to influence virulence traits in Aspergillus fumigatus. *PloS Pathog.* 7 (10), e1002330. doi: 10.1371/journal.ppat.1002330

Guirao-Abad, J. P., Weichert, A. M., Albee, A., Deck, K., and Askew, D. S. (2020). A Human IRE1 Inhibitor Blocks the Unfolded Protein Response in the Pathogenic Fungus Aspergillus fumigatus and Suggests Noncanonical Functions within the Pathway. *mSphere.* 5, 1–13. doi: 10.1128/mSphere.00879-20

Heindryckx, F., Binet, F., Ponticos, M., Rombouts, K., Lau, J., Kreuger, J., et al. (2016). Endoplasmic reticulum stress enhances fibrosis through IRE 1α-mediated degradation of miR-150 and XBP-1 splicing. *EMBO Mol. Med.* 8, 729–744. doi: 10.15252/emmm.201505925

Ishiwata-Kimata, Y., and Kimata, Y. (2023). Fundamental and applicative aspects of the unfolded protein response in yeasts. *J. Fungi.* 9, 989. doi: 10.3390/jof9100989

Kamath, M. M., Lightfoot, J. D., Adams, E. M., Kiser, R. M., Wells, B. L., and Fuller, K. K. (2023). The Aspergillus fumigatus UPR is variably activated across nutrient and host environments and is critical for the establishment of corneal infection. *PloS Pathog.* 19, 1–32 p. doi: 10.1371/journal.ppat.1011435

Kim, J. H., Cheng, L. W., Chan, K. L., Tam, C. C., Mahoney, N., Friedman, M., et al. (2020). Antifungal drug repurposing. *Antibiotics.* 9, 812. doi: 10.3390/antibiotics9110812

Kumar, A., Singh, P. K., Zhang, K., and Kumar, A. (2020). Toll-like receptor 2 (TLR2) engages endoplasmic reticulum stress sensor IRE1α to regulate retinal innate responses in S. aureus endophthalmitis. *FASEB J. Off Publ Fed Am. Soc. Exp. Biol.* 34, 13826. doi: 10.1096/fj.202001393R

Lalitha, P., Prajna, N. V., Kabra, A., and Mahadevan K, S. M. (2006). Risk factors for treatment outcome in fungal keratitis. *Opthalmology.* 113, 526–530. doi: 10.1016/j.ophtha.2005.10.063

Li, J., Li, Z., Liang, Z., Han, L., Feng, H., He, S., et al. (2018). Fabrication of a drug delivery system that enhances antifungal drug corneal penetration. *Drug Deliv.* 25, 938–949. doi: 10.1080/10717544.2018.1461278

Lightfoot, J. D., Adams, E. M., Kamath, M. M., Wells, B. L., and Fuller, K. K. (2024). Aspergillus fumigatus hypoxia adaptation is critical for the establishment of fungal keratitis. *Invest. Ophthalmol. Vis. Sci.* 65, 31. doi: 10.1167/iovs.65.4.31

Logue, S. E., McGrath, E. P., Cleary, P., Greene, S., Mnich, K., Almanza, A., et al. (2018). Inhibition of IRE1 RNase activity modulates the tumor cell secretome and enhances response to chemotherapy. *Nat. Commun.* 9, 3267. doi: 10.1038/s41467-018-05763-8

Ma, J. H., Wang, J. J., Li, J., Pfeffer, B. A., Zhong, Y., and Zhang, S. X. (2016). The role of IRE-XBP1 pathway in regulation of retinal pigment epithelium tight junctions. *Invest. Ophthalmol. Vis. Sci.* 57, 5244–5252. doi: 10.1167/iovs.16-19232

Massoudi, D., Gorman, S., Kuo, Y.-M., Iwawaki, T., Oakes, S. A., Papa, F. R., et al. (2023). Deletion of the unfolded protein response transducer IRE1α is detrimental to aging photoreceptors and to ER stress-mediated retinal degeneration. *Invest. Ophthalmol. Vis. Sci.* 64, 30. doi: 10.1167/iovs.64.4.30

Menda, S. A., Das, M., Panigrahi, A., Prajna, N. V., Acharya, N. R., Lietman, T. M., et al. (2020). Association of postfungal keratitis corneal scar features with visual acuity. *JAMA Ophthalmol.* 138, 113–118. doi: 10.1001/jamaophthalmol.2019.4852

Mimura, N., Fulciniti, M., Gorgun, G., Tai, Y.-T., Cirstea, D., Santo, L., et al. (2012). Blockade of XBP1 splicing by inhibition of IRE1α is a promising therapeutic option in multiple myeloma. *Blood J. Am. Soc. Hematol.* 119, 5772–5781. doi: 10.1182/blood-2011-07-366633

Papandreou, I., Denko, N. C., Olson, M., Van Melckebeke, H., Lust, S., Tam, A., et al. (2011). Identification of an Ire1alpha endonuclease specific inhibitor with cytotoxic activity against human multiple myeloma. *Blood J. Am. Soc. Hematol.* 117, 1311–1314. doi: 10.1182/blood-2010-08-303099

Pavlović, N., Calitz, C., Thanapirom, K., Mazza, G., Rombouts, K., Gerwins, P., et al. (2020). Inhibiting IRE1α-endonuclease activity decreases tumor burden in a mouse model for hepatocellular carcinoma. *Elife.* 9, e55865. doi: 10.7554/eLife.55865

Pierce, C. G., Uppuluri, P., Tristan, A. R., Wormley, F. L. Jr., Mowat, E., Ramage, G., et al. (2008). A simple and reproducible 96-well plate-based method for the formation of fungal biofilms and its application to antifungal susceptibility testing. *Nat. Protoc.* 3, 1494–1500. doi: 10.1038/nprot.2008.141

Price, M. O., Mehta, J. S., Jurkunas, U. V., and Price, F. W. Jr. (2021). Corneal endothelial dysfunction: Evolving understanding and treatment options. *Prog. Retin Eye Res.* 82, 100904. doi: 10.1016/j.preteyeres.2020.100904

Qiu, Q., Zheng, Z., Chang, L., Zhao, Y., Tan, C., Dandekar, A., et al. (2013). Toll-like receptor-mediated IRE1α activation as a therapeutic target for inflammatory arthritis. *EMBO J.* 32, 2477–2490. doi: 10.1038/emboj.2013.183

Richie, D. L., Feng, X., Hartl, L., Aimanianda, V., Krishnan, K., Powers-Fletcher, M. V., et al. (2011). The virulence of the opportunistic fungal pathogen aspergillus fumigatus requires cooperation between the endoplasmic reticulum-associated degradation pathway (ERAD) and the unfolded protein response (UPR). *Virulence.* 2, 12–21. doi: 10.4161/viru.2.1.13345

Richie, D. L., Hartl, L., Aimanianda, V., Winters, M. S., Fuller, K. K., Miley, M. D., et al. (2009). A role for the unfolded protein response (UPR) in virulence and antifungal susceptibility in Aspergillus fumigatus. *PloS Pathog.* 5 (1), e1000258. doi: 10.1371/journal.ppat.1000258

Ron, D., and Walter, P. (2007). Signal integration in the endoplasmic reticulum unfolded protein response. *Nat. Rev. Mol. Cell Biol.* 8, 519–529. doi: 10.1038/nrm2199

Sidrauski, C., and Walter, P. (1997). The transmembrane kinase Ire1p is a site-specific endonuclease that initiates mRNA splicing in the unfolded protein response. *Cell.* 90, 1031–1039. doi: 10.1016/S0092-8674(00)80369-4

Sircaik, S., Andes, D. R., Panwar, S. L., Román, E., Gow, N. A. R., Bapat, P., et al. (2021). The protein kinase Ire1 impacts pathogenicity of Candida albicans by regulating homeostatic adaptation to endoplasmic reticulum stress. *Cell Microbiol.* 23 (5), e13307. doi: 10.1111/cmi.13307

Stewart, C., Estrada, A., Kim, P., Wang, D., Wei, Y., Gentile, C., et al. (2017). Regulation of IRE1α by the small molecule inhibitor 4μ8c in hepatoma cells. *Cell Pathol.* 4, 1–10. doi: 10.1515/ersc-2017-0001

Sun, C. Q., Lalitha, P., Prajna, N. V., Karpagam, R., Geetha, M., O'Brien, K. S., et al. (2014). Association between *in vitro* susceptibility to natamycin and voriconazole and clinical outcomes in fungal keratitis. *Ophthalmology* 121, 1495–1500.e1. doi: 10.1016/j.ophtha.2014.03.004

Sun, H., Lin, D.-C., Guo, X., Masouleh, B. K., Gery, S., Cao, Q., et al. (2016). Inhibition of IRE1α-driven pro-survival pathways is a promising therapeutic application in acute myeloid leukemia. *Oncotarget.* 7, 18736. doi: 10.18632/oncotarget.v7i14

Thomas, P. A. (2003). Fungal infections of the cornea. *Eye.* 17, 852–862. doi: 10.1038/sj.eye.6700557

Verchot, J., and Pajerowska-Mukhtar, K. M. (2021). UPR signaling at the nexus of plant viral, bacterial, and fungal defenses. *Curr. Opin. Virol.* 47, 9–17. doi: 10.1016/j.coviro.2020.11.001

Zhang, S. X., Wang, J. J., Starr, C. R., Lee, E.-J., Park, S., Zhylkibayev, A., et al. (2023). The endoplasmic reticulum: homeostasis and crosstalk in retinal health and disease. *Prog. Retin Eye Res.* 98, 101231. doi: 10.1016/j.preteyeres.2023.101231

Zhang, L., Zhang, C., and Wang, A. (2016). Divergence and conservation of the major UPR branch IRE1-bZIP signaling pathway across eukaryotes. *Sci. Rep.* 6, 27362. doi: 10.1038/srep27362

Zhao, J., Wu, X. Y., and Yu, F. S. X. (2009). Activation of Toll-like receptors 2 and 4 in Aspergillus fumigatus keratitis. *Innate Immun.* 15, 155–168. doi: 10.1177/1753425908101521

Zhou, Y., Chen, Y., Wang, S., Qin, F., and Wang, L. (2019). MSCs helped reduce scarring in the cornea after fungal infection when combined with anti-fungal treatment. *BMC Ophthalmol.* 19, 1–11. doi: 10.1186/s12886-019-1235-6